Received: 20 March 2023 | Revised: 21 July 2023 | Accepted: 28 August 2023
DOI: 10.1111/gcb.16942

Global Change Biology WILEY

RESEARCH ARTICLE

Filter-feeding gelatinous macrozooplankton response to climate change and implications for benthic food supply and global carbon cycle

Corentin Clerc[1] | Olivier Aumont[2] | Laurent Bopp[1]

[1]LMD/IPSL, Ecole Normale Supérieure/Université PSL, CNRS, Ecole Polytechnique, Sorbonne Université, Paris, France

[2]LOCEAN/IPSL, IRD, CNRS, MNHN, Sorbonne Université, Paris, France

Correspondence
Corentin Clerc, LMD/IPSL, Ecole Normale Supérieure/Université PSL, CNRS, Ecole Polytechnique, Sorbonne Université, Paris, France.
Email: corentin.clerc@lmd.ens.fr

Present address
Corentin Clerc, École Normale Supérieure, Paris, France

Funding information
Agence Nationale de la Recherche, Grant/Award Number: ANR-17-CE32-0008; H2020 Societal Challenges, Grant/Award Number: 101003536 and 820989

Abstract

It is often suggested that gelatinous zooplankton may benefit from anthropogenic pressures of all kinds and in particular from climate change. Large pelagic tunicates, for example, are likely to be favored over other types of macrozooplankton due to their filter-feeding mode, which gives them access to small preys thought to be less affected by climate change than larger preys. In this study, we provide model-based estimate of potential community changes in macrozooplankton composition and estimate for the first time their effects on benthic food supply and on the ocean carbon cycle under two 21st-century climate-change scenarios. Forced with output from an Earth System Model climate projections, our ocean biogeochemical model simulates a large reduction in macrozooplankton biomass in response to anthropogenic climate change, but shows that gelatinous macrozooplankton are less affected than nongelatinous macrozooplankton, with global biomass declines estimated at −2.8% and −3.5%, respectively, for every 1°C of warming. The inclusion of gelatinous macrozooplankon in our ocean biogeochemical model has a limited effect on anthropogenic carbon uptake in the 21st century, but impacts the projected decline in particulate organic matter fluxes in the deep ocean. In subtropical oligotrophic gyres, where gelatinous zooplankton dominate macrozooplankton, the decline in the amount of organic matter reaching the seafloor is reduced by a factor of 2 when gelatinous macrozooplankton are considered (−17.5% vs. −29.7% when gelatinous macrozooplankton are not considered, all for 2100 under RCP8.5). The shift to gelatinous macrozooplankton in the future ocean therefore buffers the decline in deep carbon fluxes and should be taken into account when assessing potential changes in deep carbon storage and the risks that deep ecosystems may face when confronted with a decline in their food source.

KEYWORDS
benthos, carbon cycle, climate change, gelatinous zooplankton, macrozooplankton, particulate carbon, pelagic tunicates

1 | INTRODUCTION

Due to increased stratification associated with reduced surface nutrient supply, net primary production (NPP) is projected to decrease by 3.00±9.10% by the end of the century under the SSP5.85 high emission scenario (Cooley et al., 2022; Kwiatkowski et al., 2020). As a consequence, zooplankton biomasses are projected to decrease by 9.0±8.9% by the end of the century (Cooley et al., 2022) due to trophic amplification and reduced transfer efficiency (Kwiatkowski et al., 2019; Stock et al., 2014).

Yet, in contrast with the overall projected decline in total zooplankton biomass, many studies assert that gelatinous zooplankton might increase globally as a result of climate change (Brotz et al., 2012; Condon et al., 2012, 2013; Gibbons & Richardson, 2013; Purcell, 2012; Richardson et al., 2009). Several factors are likely to influence gelatinous zooplankton abundance under climate change: warming (Condon et al., 2012, 2014; Lucas et al., 2014; Pitt et al., 2014; Purcell, 2012), hypoxic and eutrophic conditions (Purcell et al., 2007), and acidification (Pitt et al., 2018; Richardson et al., 2009; Richardson & Gibbons, 2008). Impacts may be direct, or indirect via a competitive advantage over directly impacted organisms (Acuña et al., 2011; Francis et al., 2012; Roux et al., 2013). Nevertheless, there is a clear lack of observational data on these organisms and a large uncertainty about the mechanisms involved.

Compared with carnivorous gelatinous macrozooplankton (e.g., hydrozoans, scyphozoans, cubozoans, and ctenophores), on which most studies have focused, filter-feeding gelatinous macrozooplankton (FFGM; e.g., salps, pyrosomes, and doliolids) have been particularly neglected (Henschke et al., 2016). Beyond direct physiological impacts which are solely documented, FFGM may be favored by changes in the planktonic ecosystem structure. Associated with a climate change-induced decrease in NPP, marine ecosystem models project a decrease in the average body size of phytoplankton (Peter & Sommer, 2013) and zooplankton, as low-productive environments favor smaller body sized organisms (Armengol et al., 2019). As recently suggested by Heneghan et al. (2023) using a model representing nine zooplankton groups, including salps and larvaceans, FFGM could replace other macrozooplankton organisms (e.g., krill and large copepods; Everett et al., 2022) due to their high clearance rate (Acuña et al., 2011), their access to prey up to five orders of magnitude smaller than themselves (Sutherland et al., 2010; Sutherland & Thompson, 2022), and their ability to exploit low-chlorophyll environments (Clerc, Bopp, Benedetti, et al., 2023; Luo et al., 2022; Sutherland & Thompson, 2022). Climate change has the potential to alter the composition of zooplankton and consequently their role in marine biogeochemical cycles (Chelsky et al., 2015; McKinley et al., 2017; Steinberg & Landry, 2017) and in the regulation of upper trophic levels (UTLs; Dupont et al., 2022; Heneghan et al., 2023).

Because of their rapidly sinking carcasses and fecal pellets, large zooplankton (Stamieszkin et al., 2015), and in particular gelatinous zooplankton (Henschke et al., 2016; Lebrato et al., 2013), are more likely to efficiently transport particulate organic carbon (POC) to the seafloor. "Jelly-falls", defined as the sinking of gelatinous zooplankton carcasses in the water column following a swarming event, can result in the export of huge amounts of organic matter to the seafloor (Lebrato et al., 2012, 2019; Luo et al., 2020; Sweetman et al., 2014; Sweetman & Chapman, 2015). In particular, recent studies suggest that FFGM may play a central role in deep ocean carbon fluxes (Clerc, Bopp, Benedetti, et al., 2023; Décima et al., 2023; Henschke et al., 2016; Luo et al., 2022; Steinberg et al., 2023). Their role in the carbon cycle in a changing climate remains unknown.

Fluxes of POC to the deep ocean are the primary source of food for benthic organisms (McClain et al., 2012). Because most benthic communities are limited by food supply (Young et al., 1994) and because there is a positive relationship between primary production and this supply (Smith et al., 2008), benthic communities are likely to be negatively affected by climate change (Cooley et al., 2022). Indeed, model-based studies agree in projecting a global decrease in particulate carbon fluxes to the seafloor (DeVries et al., 2017; Sweetman et al., 2017) resulting in a reduction in benthic biomass (Jones et al., 2014; Yool et al., 2017). Nevertheless, current estimates of POC fluxes to the deep ocean are based on Earth System Models (ESM) that do not include macrozooplankton and thus large organic matter particles (Sweetman et al., 2017; but see Luo et al., 2022 for upper ocean export). As important potential contributors to the flux of POC to the seafloor (Clerc, Bopp, Benedetti, et al., 2023), and thus as a potentially essential source of food for the benthos (Ates, 2017; Smith et al., 2016; Sweetman et al., 2014; van der Reis et al., 2020), a proper assessment of the impacts of macrozooplankton, and in particular of FFGM, on these fluxes in a changing climate could provide key insights on future changes in benthic ecosystems.

In this study, we present a first analysis of the projected response to climate change in a spatially resolved biogeochemical model that explicitly represents FFGM and their interaction with the carbon cycle through the entire water column. The model used here is PISCES-FFGM (Clerc, Bopp, Benedetti, et al., 2023), a revised version of Pelagic Interactions Scheme for Carbon and Ecosystem Studies volume 2 (PISCES-v2; Aumont et al., 2015) that includes one FFGM group and one crustacean-like generic macrozooplankton group. We ran the model across the historical period (1850–2005) and both the RCP8.5 and RCP2.6 scenarios (2006–2100) using output from the IPSL-CM5A-LR ESM (Dufresne et al., 2013). When analyzing these biogeochemical projections, we investigated how the trophic structure will be affected by climate change when considering two macrozooplankton groups with a particular focus on the potential future shift from crustaceans to gelatinous zooplankton organisms. We then evaluated how the impacts of climate change on macrozooplankton biomass and composition will affect the benthic food supply as macrozooplankton are key players for deep particulate carbon export. Lastly, we explored the potential effect of gelatinous and nongelatinous macrozooplankton representation on how the carbon cycle will be affected by climate change.

2 | MATERIALS AND METHODS

2.1 | Model and configuration

The marine biogeochemical model used in the present study is PISCES-FFGM (Clerc, Bopp, Benedetti, et al., 2023), a revised version of PISCES-v2 (Aumont et al., 2015) that explicitly accounts for macrozooplankton. PISCES-v2 includes five nutrient pools (Fe, NH_4^+, Si, PO_4^{3-}, and NO_3^-), two phytoplankton groups (diatoms and nanophytoplankton), two zooplankton groups (one micro- and one mesozooplankton group), and an explicit representation of particulate and dissolved organic matter, reaching a total of 24 prognostic variables (tracers).

In PISCES-FFGM, two groups of macrozooplankton were added, one corresponding to generic macrozooplankton organisms (hereafter referred to as GM) and the other to salp-like FFGM organisms (hereafter referred to as FFGM). In addition to their carbon biomass, three additional tracers were introduced into the model for each macrozooplankton group corresponding to fecal pellets in carbon and iron units and carcasses in carbon units (GM Carcasses, GM Fecal Pellets, FFGM Carcasses and FFGM Fecal Pellets, see Figure S1).

Because PISCES-FFGM explicitly represents the macrozooplankton carcasses and fecal pellets, it accounts for the high sinking velocities of these detritus that result in an efficient POC export to the deep sea. It also explicitly represents the filtration behavior of FFGM, which implies a different diet composition than that of generic macrozooplankton (Figure S1), resulting in a different trophic response to ecosystem composition in the two compartments (GM and FFGM).

Here, we use PISCES-FFGM, embedded in the Nucleus for European Modeling of the Ocean (NEMO) within a global ocean configuration and in "offline" mode, that is, forced with already existing ocean physical fields (e.g., temperature, salinity, and ocean currents). To reduce computational costs, we use the coarse-resolution ORCA2 configuration from NEMO, with a horizontal resolution of 2°×2°cos(latitude), increased latitudinally to 0.5° at the equator, and 31 vertical levels with vertical resolution decreasing with depth (Madec, 2008).

A full description of the model and its parameterizations is provided in Clerc, Bopp, Benedetti, et al. (2023).

2.2 | Experimental design

We use three different versions of PISCES-FFGM: (1) the standard version with the same parameter values as in Clerc, Bopp, Benedetti, et al. (2023), hereafter called PISCES-FFGM, (2) a version in which FFGM growth rate is set to 0 so that GM only can grow, hereafter called PISCES-GM, and (3) a version in which both FFGM and GM growth rates are set to 0 so that tracers dynamics is similar to that of PISCES-v2 (Aumont et al., 2015), hereafter called PISCES-v2. The comparison of PISCES-FFGM versus PISCES-GM allows to quantify the effect of including FFGM, while PISCES-v2 versus PISCES-GM comparison allows to quantify the effect of including macrozooplankton.

We use these three versions in forced offline mode with monthly fields from the IPSL-CM5A-LR ESM (Dufresne et al., 2013), for both historical (1850–2005) and future (2006–2100) periods. The choice of IPSL-CM5A-LR that was used for CMIP5 (fifth phase of the Coupled Model Intercomparison Project, Taylor et al., 2012), instead of IPSL-CM6A-LR (Boucher et al., 2020) used for CMIP6 (sixth phase of the Coupled Model Intercomparison Project, Eyring et al., 2016), was dictated by our decision to use the coarse-resolution ORCA2 grid. Indeed, using outputs from the ocean component of IPSL-CM6A-LR on the eORCA1 grid (1° horizontal resolution and 75 vertical levels) would have increased the CPU cost of our simulations by 15.

The climate projections follow two scenarios: (1) a high emission pathway, namely Radiative Concentration Pathway 8.5 (RCP8.5), a scenario in which the radiative forcing steadily increases to 8.5 $W\,m^{-2}$ in 2100 due to high greenhouse gas emissions and (2) a low emission pathway, namely Radiative Concentration Pathway 2.6 (RCP2.6), in which the radiative forcing reaches 2.6 $W\,m^{-2}$ (Moss et al., 2010). Note that if we had used outputs from IPSL-CM6A under ssp5-8.5, the qualitative effects of including FFGM and GM on the ecosystem structure and on the carbon cycle under a climate-change scenario would probably have been quite similar to the ones discussed here, as suggested in Bopp et al. (2022) for NPP and plankton biomass responses using a similar PISCES version under RCP8.5 using IPSL-CM5A forcing and under ssp5-8.5 within IPSL-CM6A-LR.

In parallel to the historical and projection simulations, we also run a 250-year control simulation with preindustrial climate and atmospheric CO2 for the three model configurations PISCES-v2, PISCES-GM, and PISCES-FFGM. This enables to estimate anthropogenic carbon uptake and storage and to check for any inherent drifts in the simulations. These simulations are called pi-control runs.

In detail, PISCES-FFGM is run first for 500 years with a monthly climatological forcing as described in Clerc, Bopp, Benedetti, et al. (2023). Starting from this last run, PISCES-FFGM, PISCES-GM, and PISCES-v2 are then run for 100 years with preindustrial climate and atmospheric CO_2 forcing. The pi-control and historical/projections simulations are branched from these 100 years of short spin-up simulations. A schematic representation of the experimental design is presented in Figure S2.

2.3 | Analysis of model outputs

Consistent with the convention from the latest IPCC reports (AR6 WG1 and WG2), two time periods have been defined to calculate the anomalies. The "present-day" (PD) period (1995–2014) is used as a reference. The "long-term" (LT) period (2081–2100) characterizes the state of the system at the end of the century. With the exception of time series, the results presented are averaged over the 20 years of each period.

In order to compensate for any internal drift in the system (which is found to be very small, especially for surface ocean fields), the fields presented in this study are corrected with the pi-control runs. For spatially averaged analyses (e.g., global and by-region means), a linear regression is calculated on the evolution of the considered variable over time in the pi-control run. The obtained trend is then removed from the variable in the historical/projection run. For other analyses (e.g., maps and zonal averages), the LT-PD (2081–2100 vs. 1995–2014) anomaly calculated for the considered variable in the pi-control is removed from the LT-PD anomaly of the climate-change run.

In order to analyze the PISCES-specific spatial structure of biomasses response to climate change (Figure S3), five regions are defined for the regional analysis (Figure 1b), based on latitudes and on the distribution of surface chlorophyll in the PISCES-FFGM present-day climatology. High-latitude regions are as follows: the Southern Ocean (SO) defined as waters south of 50°S and the Arctic Ocean (AO) defined as waters north of 60N. The definition of low and mid-latitude regions is based on annual mean chlorophyll concentrations: areas with values below 0.07 mg Chl m^{-3} constitute the low-chlorophyll region (LC), areas with values between 0.07 and 0.25 mg Chl mm^{-3} constitute the intermediate chlorophyll region (IC), and areas with values higher than 0.25 mg Chl mm^{-3} constitute the high-chlorophyll region (HC). Note that similar regional analysis have been performed based on the three biomes used in Luo et al. (2022; see Figure S4), but that this spatial separation did not capture the specific response of PISCES biomass at high latitude (see Section 3.1.1).

To focus on implications for deep benthos, we limit the analyses of organic matter fluxes at the ocean floor (Section 3.2) to areas where depth is greater than 1000 m.

3 | RESULTS

3.1 | Pelagic ecosystem

3.1.1 | Biomasses and trophic structure

PISCES-FFGM projects a strong biomass decline for all organisms under the RCP8.5 scenario, but with an important trophic amplification (Table 1, Figure 1a). The integrated biomass across all trophic levels in the upper 300 m of the ocean is projected to decline by 8.7% at the end of the 21st century (LT, 2081-2100) relative to present day (PD, 1995–2014). Phytoplankton biomass decreases by 4.5% while zooplankton biomass decreases by 12.8%, consistent with the trophic amplification hypothesis (Chust et al., 2014; Kwiatkowski et al., 2019). Within zooplankton, the decline increases with trophic level (TL): −9.3% for microzooplankton (TL = 2), −12.0% for FFGM (TL = 2.2), −14.0% for mesozooplankton (TL = 2.4), and −15.1% for GM (TL = 3.3); Table 1, Figure 1a. Because of their filter-feeding mode, which shortens the food chain and gives them access to preys less affected by climate change, the decline in FFGM is not only less than that of GM, which have the same body size, but also less than that of mesozooplankton, which are smaller. Thus, although FFGM decline is larger than the estimated available food decline

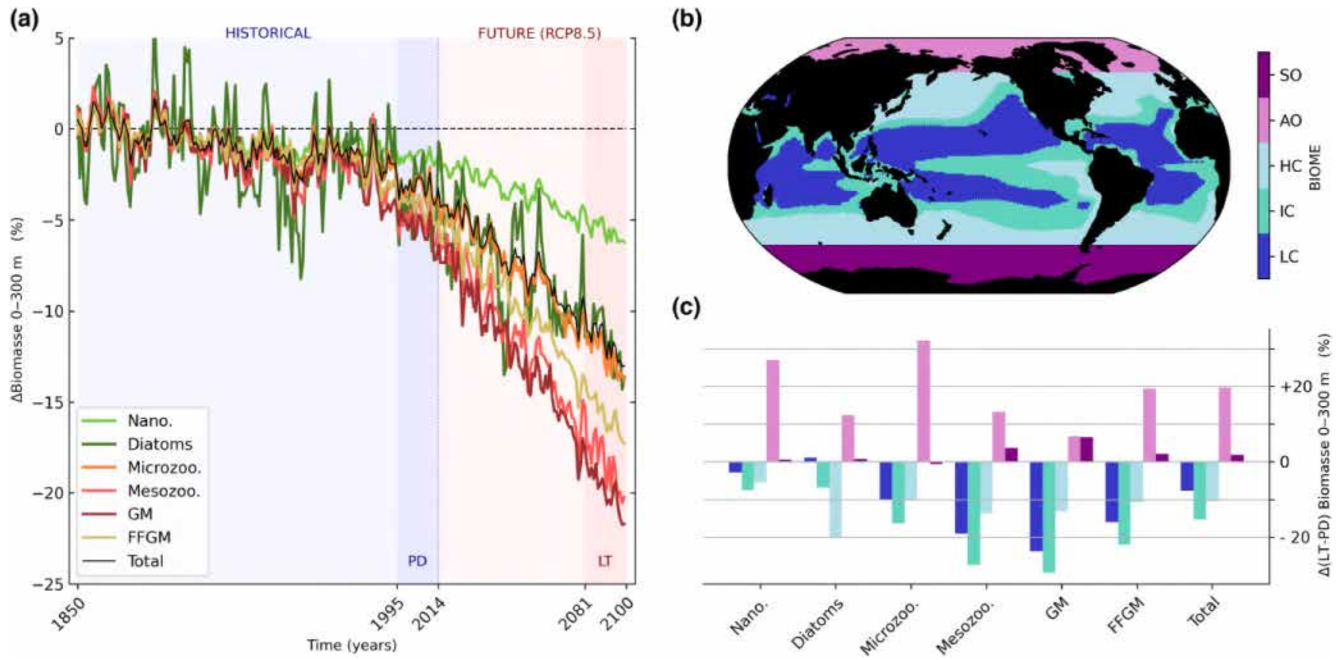

FIGURE 1 Mean global and regional changes in PISCES-FFGM phyto- and zooplankton biomasses under historical and RCP8.5 scenario. (a) Time series of upper 300 m mean global biomass anomalies relative to 1850–1900 preindustrial values. PD and LT indicate present-day (1995–2014) and long-term (2081–2100) reference periods, respectively. (b) Spatial distribution of the different regions (see Section 2.3 for their definition). (c) Regional anomalies in LT biomass averaged over the top 300 m, by region, relative to the PD.

TABLE 1 Mean global ecosystem biomasses and trophic structure over 1995–2100 for RCP8.5.

Group of organisms	Nanophytoplankton	Diatoms	Microzooplankton	Mesozooplankton	GM	FFGM	Total
Biomass PD (TgC)	626	85	162	386	84	93	1435
Change in biomass LT-PD (%)	−4.1	−7.9	−9.3	−14.0	−15.1	−12.0	−8.7
Relative abundance PD (−)	0.4363	0.0592	0.1128	0.2686	0.0585	0.0646	1
Change in relative abundance LT-PD (−)	+0.0222	+0.0005	−0.0007	−0.0155	−0.0041	−0.0023	
Trophic level PD	1	1	2	2.4264	3.3352	2.2145	
Change in trophic level LT-PD	0	0	0	−0.0005	−0.0013	−0.0001	
Grazing PD (proportion of NPP)			0.7796	0.4054	0.0222	0.0297	
Change in grazing LT-PD (%)			+1.64	−2.71	−6.66	−2.59	

Note: Biomasses, relative abundances, trophic levels, and grazing fluxes are computed for the present day (PD; 1995–2014). Changes are computed as the difference between long-term (LT; 2081–2100) and present-day values. They are expressed in % for biomass and grazing, while absolute values are given for relative abundance and trophic level changes. Note that grazing fluxes are expressed as proportion of the global net primary production (NPP; 36.91 PgC year^{-1} for PD, 33.62 PgC year^{-1} for LT). All values are integrated over the upper 300 m.

Abbreviations: GM, generic macrozooplankton; FFGM, filter-feeding gelatinous zooplankton.

(computed as the preference-weighted sum of all preys) of −5.4% which reveals a trophic amplification (Figure S5), FFGM are less sensitive to climate change than meso- and macrozooplankton at the global scale.

Those organism-dependent climate-change impacts induce slight changes in the biomass structure: the "gelatinous pathway" (i.e., energy that flows through microzooplankton and FFGM) is favored over the "crustacean pathway" (i.e., energy that flows through mesozooplankton and GM). Indeed, while total grazing by crustaceans is reduced by 2.7% and 6.7% for mesozooplankton and GM, respectively, grazing fluxes for the gelatinous pathway are less affected: FFGM grazing flux is reduced by 2.6% and microzooplankton one even increases by 1.6% (Table 1). In terms of relative composition, the contribution of plankton types to the total planktonic biomass decreases by −1% and −4% for microzooplankton and FFGM, respectively, while it decreases by −6% and −7% for mesozooplankton and GM, respectively (Table 1).

However, neither zooplankton-specific diet composition (Figure 2) nor estimated trophic levels (Table 1 and Figure S6) are significantly affected by climate change (TL global changes <0.1%, diet global composition changes <1%). Consequently, while our model projects significant impacts on biomass (Figure 1) and on absolute grazing fluxes (Table 1), it does not show significant changes in the trophic structure of the ecosystem. The results are therefore presented here assuming that the trophic structure of the ecosystem remains constant over time.

A regional analysis reveals a strong regional variability of these climate-change effects on the ecosystem structure (Figure 1b,c). In high-latitude regions (AO and SO), total biomasses increase by +19.6% and +1.8% in the AO and SO, respectively. The trophic structure of the anomalies is however different between the two regions: in the Southern Ocean, which is highly productive (mean chlorophyll at 0.43 mg Chl m^{-3}), crustaceans (mesozooplankton and GM) are favored over microzooplankton and FFGM (Figure 1c). In the Arctic, which is less productive (mean 0.28 mg Chl m^{-3}), it is the opposite (Figure 1c). In tropical and temperate regions (LC, IC and HC), total biomasses decline (LC −7.7%, IC −15.4% and HC −10.5%, Figure 1c). In LC and IC, anomalies follow the global pattern with a strong trophic amplification. The effect is greatest in IC, where biomasses decrease by on average 7% more than in LC (Figure 1c). This greatest sensitivity is due to a partial switch from historical IC to future LC (Figure 4b). The effect of climate change is more moderate in HC with the exception of a strong decline in diatom biomass (Figure 1c). In IC and LC, microzooplankton and FFGM biomass decline less than that of mesozooplankton and GM, and diatoms, which represent less than 10% of total phytoplankton biomass, are slightly less affected than nanophytoplankton (Figure 1c).

Under the RCP2.6 scenario, PISCES-FFGM projects a lower 0–300 m biomass decline (LT-PD change of −1.2%), but similar trophic amplification patterns to the RCP8.5 scenario (Figure S7). Overall, the relationship between macrozooplankton biomass trends and global surface warming is consistent between the two RCP scenarios and the historical period (Figure 3a): GM decline (−3.54 ± 0.03% per degree of warming) is one quarter higher than FFGM decline

FIGURE 2 Mean current and future global annual zooplankton diet in PISCES-FFGM for the present day (PD; 1995–2014, upper panels) and for the end of the 21st century under RCP8.5 (LT; 2081–2100, lower panels). All are expressed in % of the total diet and in absolute carbon fluxes in TgC year^{-1}.

(−2.79 ± 0.02% per degree of warming). Note that GM decline is similar in the PISCES-GM simulation (−3.57 ± 0.03% per degree of warming, Figure 3a), so the inclusion of FFGM has no or little impact on the projected GM decline under climate change.

3.1.2 | Macrozooplankton composition

Due to their filter-feeding mode of predation that shortcuts the food chain, FFGM decline less than GM. Indeed, the trophic amplification is significantly reduced for this group. Considering the relationship between macrozooplankton composition and chlorophyll levels, we relate changes in ecosystem composition with environmental changes.

At PD, FFGM dominate macrozooplankton in low-productive areas of tropical and temperate latitudes. As shown in Figure 4a, the chlorophyll iso-contour corresponding to 0.07 mg Chl m^{-3} approximatively delineates the regions where the FFGM:GM ratio is greater than 1. In the long term, the link between low-chlorophyll waters and high FFGM:GM ratio is conserved (Figure 4b). This pattern partially explains the difference in the overall variations in GM and FFGM (Figure 3a). In Figure 4b (RCP8.5) and in Figure S8b (RCP2.6), the black contour indicates a FFGM:GM ratio of 1.4, arbitrarily chosen to provide the best fit with the chlorophyll contour. The projected future extension of the area within this contour (solid vs. dotted line) indicates a 32% extension of the area where the ratio exceeds this value (PD area: 1.11 x 10^8 km^2, LT area: 1.47 x 10^8 km^2). Similarly, the chlorophyll contours indicate a 38% extension of low-productive areas (solid vs. dotted green lines; PD area: 1.11 x 10^8 km^2, LT area: 1.52 x 10^8 km^2). Even in HC areas where GM dominates, the FFGM:GM ratio is increasing due to declining productivity and biomasses (Figure 1c and Figure S7c). In AO, productivity is increasing but is still low enough so that FFGM are favored and FFGM:GM ratio increases. The only exception is the SO where productivity is already high and is projected to further increase. This favors GM, so that the FFGM:GM ratio decreases in this region. Thus, globally there is an extension of the areas of FFGM dominance due to the extension of the low-productivity areas.

3.2 | POC export fluxes

3.2.1 | Global changes in POC export fluxes at 100 and 1000 m

Changes in particulate organic carbon (POC) sinking fluxes are largely driven by changes in surface productivity. Under the RCP8.5 scenario, the decreases in POC fluxes at 100 m depth for PISCES-FFGM and PISCES-GM are similar, −16.9% and −17.2%, respectively (Table 2, Table S3 and Figure 5a,b). PISCES-v2 shows a lower sensitivity to climate change with a decline of −14.3% (Table S4 and Figure 5c), which can be related to a different ecosystem structure projected by PISCES-v2 compared with the two other model configurations (Table 1, Tables S1 and S2). At 1000 m, the export flux decreases by −15.9%, −17.3% and −18.0% for PISCES-FFGM, PISCES-GM, and PISCES-v2, respectively (Table 2, Tables S3 and S4 and Figure 5a–c). Differences are particularly important in low-productive oligotrophic areas (LC in Table S5) where the decrease in POC fluxes is attenuated by 6% in PISCES-GM and by 12% in PISCES-FFGM compared with PISCES-v2 (decrease of −32% at the end of the 21st century, see Table S5). The dampened anomaly at 1000 m compared to 100 m in PISCES-FFGM simulations is mostly explained by the higher contribution of FFGM carcasses and fecal pellets, less affected by climate change than other particles, to the deeper POC flux. For the same reason, the 1000 m POC flux decline is higher in PISCES-GM than in PISCES-FFGM.

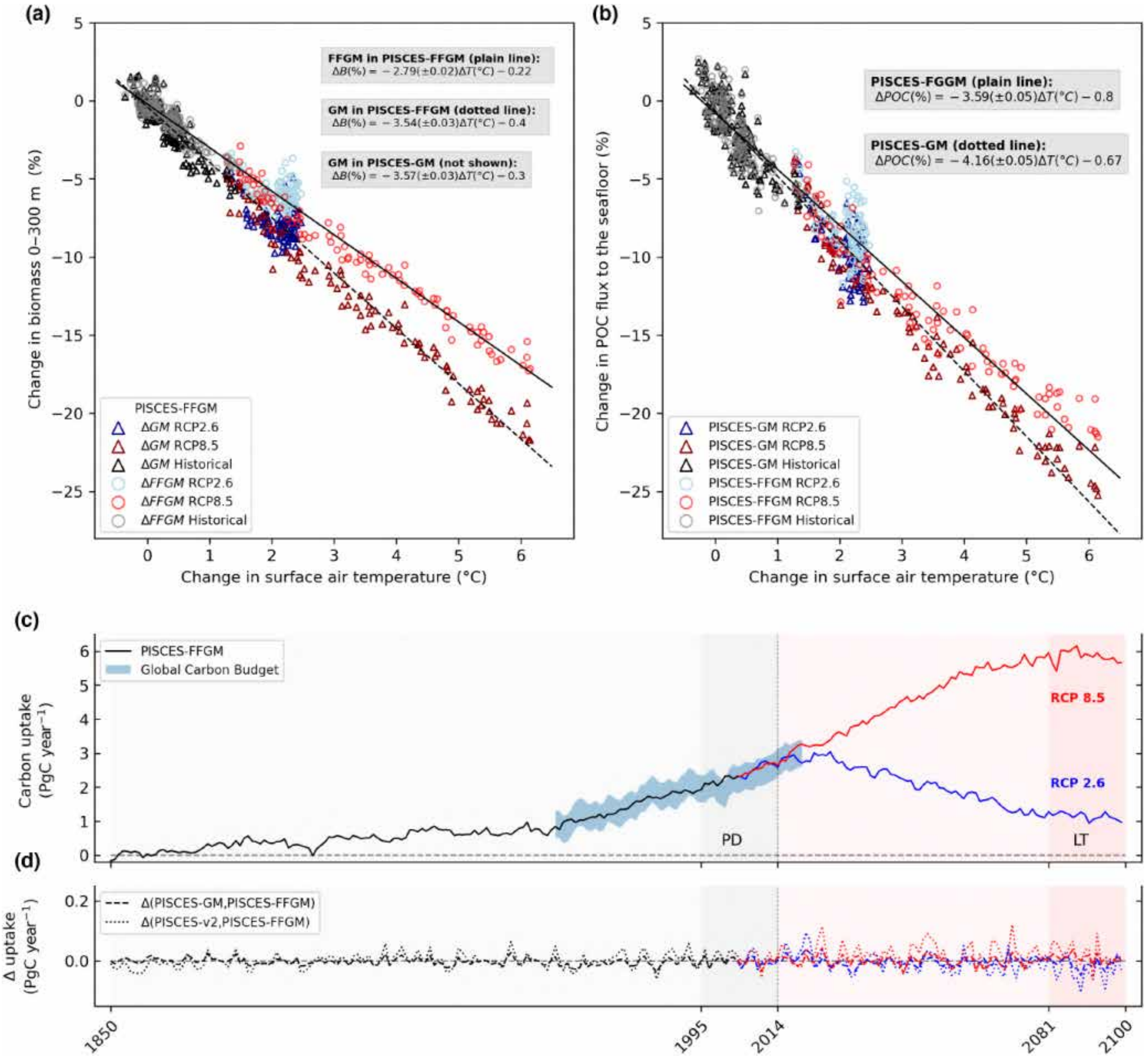

FIGURE 3 Projected changes in macrozooplankton biomass and their impacts on carbon fluxes and carbon uptake under RCP8.5 and RCP2.6 scenarios. (a) Projected trends of PISCES-FFGM upper 300 m mean GM and FFGM biomass in relation to global air temperature changes since preindustrial times (1850–1900). Gray boxes show the relationships estimated with linear regression fits. The slope is a proxy for biomass change per degree of warming. (b) Projected trends of PISCES-FFGM and PISCES-GM POC export at the seafloor (>1000 m) as a function of global air temperature changes since preindustrial times (1850–1900). Gray boxes show the relationship estimated from linear regression fits. The slope is a proxy of export flux change per degree of warming. (c) Time series of the mean anthropogenic carbon uptake (PgC year^{-1}). Shaded area is the Global Carbon Budget 2021 ocean sink product (uncertainty of ±0.4 PgC year^{-1} on average) and is estimated from the average of eight global ocean biogeochemistry models (including NEMO-PISCES) and the average of seven ocean fCO_2 data products (Friedlingstein et al., 2022). PD and LT indicate present-day (1995–2014) and long-term (2081–2100) reference periods. (d) Time series of the annual differences in mean anthropogenic carbon uptake (PgC year^{-1}) for PISCES-v2 and PISCES-GM compared with PISCES-FFGM.

3.2.2 | Global changes in seafloor POC fluxes and impact on benthos

POC is an important source of food for the benthos. Since macrozooplankton, and in particular FFGM, are important contributors to deep export (Clerc, Bopp, Benedetti, et al., 2023; Luo et al., 2020), their representation in a model could affect the simulated amount of organic carbon reaching the sea floor and thus have potential implications for benthic communities. As shown in Figure 5a, organic carbon export declines twice as much as the total biomass in PISCES-FFGM: at 100 m it decreases by 16.9% during LT compared with PD (Table 2). This translates into a 14.9% decrease in total POC flux to

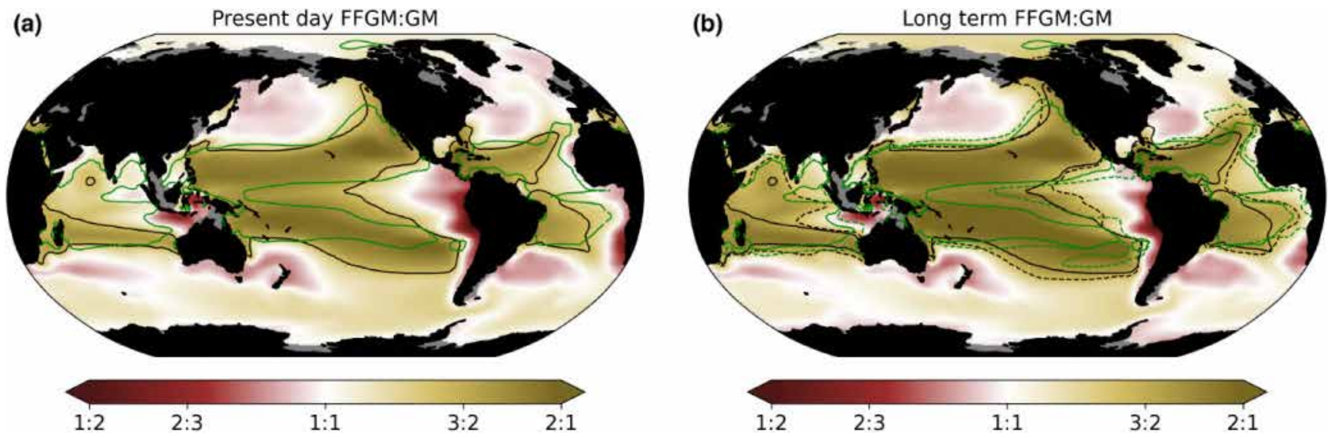

FIGURE 4 Historical and RCP8.5 future FFGM:GM ratios. (a) Present day (1995–2014) and (b) long term (2081–2100). Yellow tones indicate FFGM dominance, whereas red tones indicate GM dominance. Dark green lines indicate 0.07 mg Chl m^{-3} iso-chlorophyll concentration (plain lines for present day and dotted lines for long term). Black lines indicate 1.4 iso-FFGM:GM ratio (plain lines for present day and dotted lines for long term).

TABLE 2 Mean global particulate organic carbon (POC) fluxes and particle composition over the 1995–2100 period under RCP8.5 scenario.

		All organisms		GM		FFGM		
Depth	**Value**	**Small**	**Large**	**Ca.**	**FP**	**Ca.**	**FP**	**Total POC**
100 m	Flux PD (TgC $year^{-1}$)	2416	4254	94	169	133	282	7348
	Change in flux LT-PD (%)	−14.5	−18.4	−19.5	−20.7	−13.7	−14.6	−16.9
	Contribution to total POC flux (–)	0.3288	0.5790	0.0127	0.0230	0.0180	0.0384	1
	Change in contribution LT-PD (–)	+0.0095	−0.0099	−0.0004	−0.0010	+0.0007	+0.0011	
1000 m	Flux PD (TgC $year^{-1}$)	116	1184	117	151	153	278	2000
	Change in flux LT-PD (%)	−19.1	−16.3	−16.4	−18.9	−11.0	−13.3	−15.9
	Contribution to total POC flux (–)	0.0582	0.5919	0.0587	0.0756	0.0766	0.1391	1
	Change in contribution LT-PD (–)	−0.0023	−0.0033	−0.0004	−0.0027	+0.0045	+0.0042	
Seafloor (>1000 m)	Flux PD (TgC $year^{-1}$)	14	134	87	71	121	217	643
	Change in flux LT-PD (%)	−23.3	−16.5	−16.9	−19.6	−11.1	−13.2	−14.9
	Contribution to total POC flux (–)	0.0213	0.2075	0.1350	0.1109	0.1879	0.3373	1
	Change in contribution LT-PD (–)	−0.0021	−0.0038	−0.0032	−0.0062	+0.0085	+0.0067	

Note: Fluxes and contributions are computed for the present day (PD; 1995–2014). Changes are computed as the difference between long-term (LT; 2081–2100) and present-day values. They are expressed in % for fluxes, while absolute values are given for relative contribution changes.

Abbreviations: FFGM, filter-feeding gelatinous zooplankton; GM, generic macrozooplankton.

the seafloor. While at 100 m, small and large particles together represent 90% of the total exported organic matter (Table 2), and thus dominate the flux changes (Figure 6b), at the seafloor, macrozooplankton (GM + FFGM) carcasses and fecal pellets become dominant at 75% (Table 2) and drive the flux changes (Figure 6d). Therefore, macrozooplankton drive climate-change impacts on benthic particulate food supply.

The attenuation of the flux decline at the seafloor relative to the surface (by 2%, Table 2) is explained by two mechanisms: (1) organisms living below 100 m are less affected by climate change than those living at the surface (12.5% biomass decline between 0 and 100 m vs. 2.1% biomass decline between 100 and 300 m). It induces lower seafloor anomalies of large particles, carcasses, and fecal pellets fluxes than at 100 m (1%–2%, Table 2). Note that the small particle flux decline is larger at the seafloor than at 100 m but the effect is negligible on total anomalies, as they only account for a few % of this decline at the seafloor (Table 2). (2) FFGM-produced particles are less affected by climate change than other types of particles and their contribution to POC flux increases with depth. Indeed, the flux of FFGM carcasses and fecal pellets, accounting for 43% of the total POC export decline at the seafloor (compared to 5% at 100 m), decreases by 11% and 13%, respectively, while other particle fluxes decrease by more than 16% at the seafloor (Figure 6b,e, Table 2).

Of these two processes, the second one is the more important in explaining the dampened decline at the sea floor compared to 100 m:

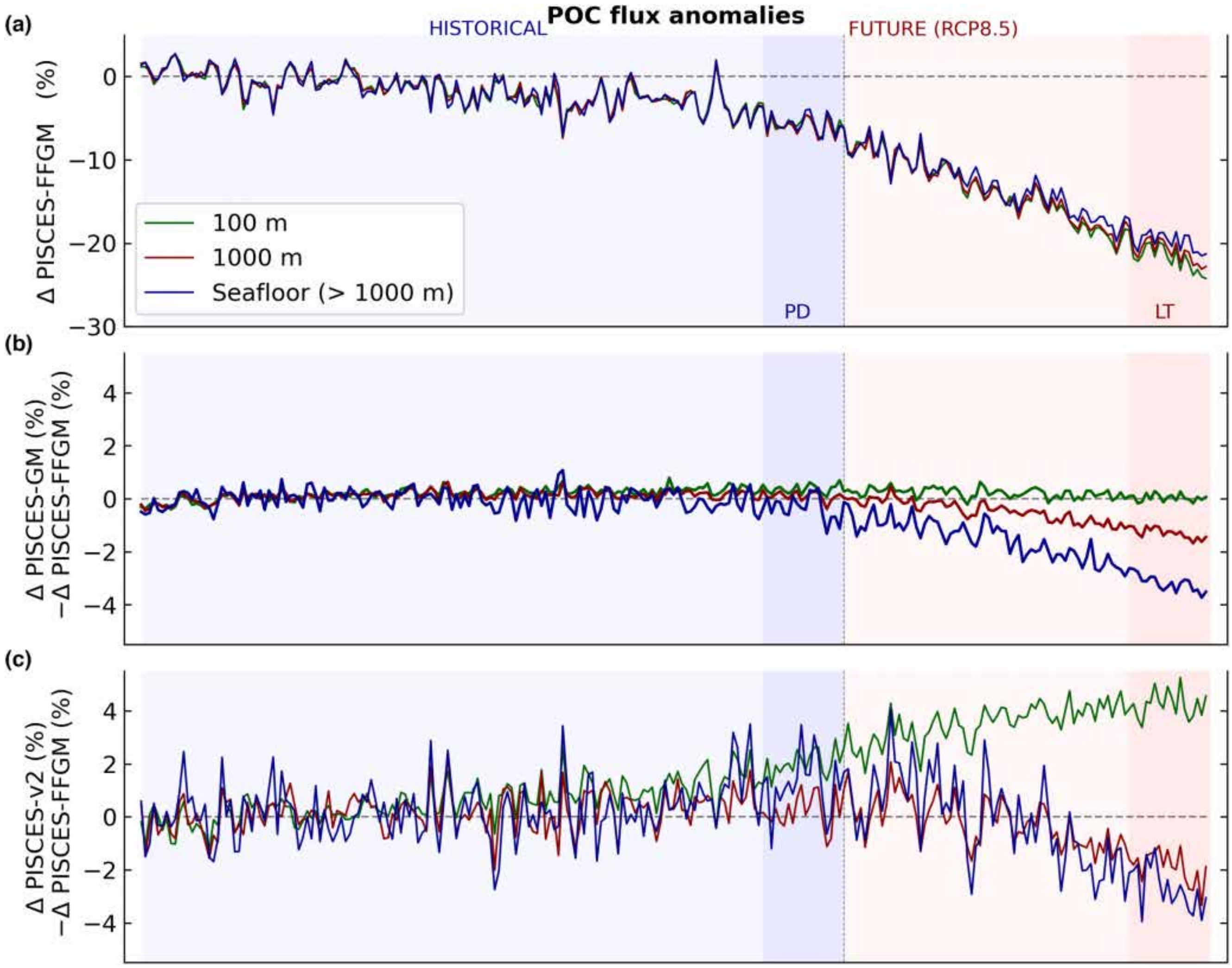

FIGURE 5 Evolution of particulate organic carbon export under RCP8.5 scenario. (a) Time series of the mean global anomalies (%) of PISCES-FFGM POC export at 100, 1000 m and to the seafloor relative to 1850–1900 preindustrial values. (b) (resp. [c]) Time series of the difference between PISCES-GM (resp. PISCES-v2) and PISCES-FFGM mean global POC export anomalies (%) at the same horizons. The color code for the different depth horizons is the same as in panel (a).

when FFGM are removed, as in PISCES-GM, the export decline at 100 m is similar, but the export decline at the seafloor is 3.0% higher in PISCES-GM than in PISCES-FFGM and thus reaches values similar to those modeled at 100 m (Figure 5b and Table S3). Consistently, when considering RCP8.5, RCP2.6 and historical export trend in response to global air temperature changes (Figure 3b), the decline in export to the seafloor simulated with PISCES-GM (−4.16 ± 0.05% per degree of warming) is 16% higher than the decline in export to the seafloor simulated with PISCES-FFGM (−3.59 ± 0.05% per degree of warming).

3.2.3 | Spatial patterns

Under the RCP8.5 scenario, seafloor and 100 m POC flux anomalies display contrasting spatial patterns. Figure 6a–c shows the POC flux anomalies at 100 m. The pattern driving the sign of this anomaly is the same as that described for the biomass anomalies: export increases at high latitudes (AO and SO, Table S5, Figure 6b) and decreases at mid and low latitudes (LC, IC, and HC, Table S5, Figure 6b). However, since high-latitude regions (AO and SO) contribute to 15% of total PD export flux, it results in a significant export decrease at the global scale (Figure 5a, Table 2). At the seafloor, the sign of the anomaly is mostly similar (Figure 6d–f) and we do not focus on the areas where the sign of the anomaly is opposite because they represent a negligible area at the global scale (interval between the solid and dashed lines in Figure 6d). Areas where the seafloor anomaly is attenuated relative to 100 m anomaly are located in the oligotrophic gyres as well as in the Arctic. FFGM dominate in these regions. Areas where the seafloor anomaly is amplified relative to the surface (positive amplification in the SO, negative amplification in the North Pacific and the North Atlantic) correspond to regions where GM dominate (Figure 6a,c,d,f). When removing FFGM in PISCES-GM (dashed line), the same zonal pattern of amplification/attenuation of POC flux

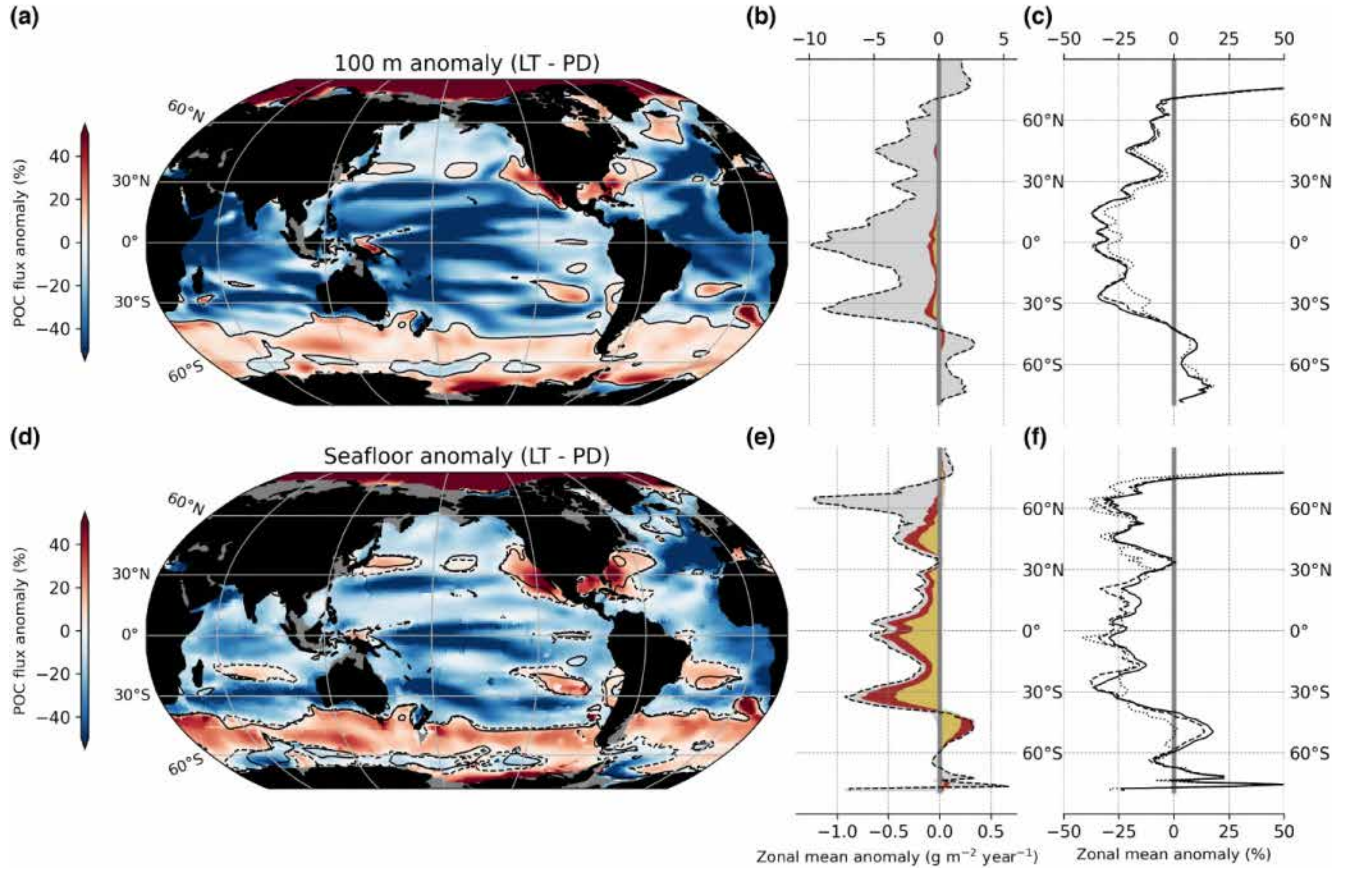

FIGURE 6 Global and zonally averaged POC flux anomalies for LT (2081–2100) versus PD (1995–2014) for the PISCES-FFGM RCP8.5 simulation. Anomaly (%) computed (a) at 100 m and (d) at the seafloor (>1000 m). Black lines indicate the limits between positive and negative anomalies at 100 m (plain) and at the seafloor (>1000 m, dotted). (b) and (e) Zonal mean absolute anomalies computed (b) at 100 m and (e) at the seafloor (gC m^{-2} $year^{-1}$). The dashed line shows the anomaly for total POC. The fill colors show the contribution of the different components of the POC: small and medium particles in gray, GM carcasses and fecal pellets in red, and FFGM carcasses and fecal pellets in yellow. (c) and (f) Zonal mean anomalies (%) at 100 m and at the seafloor, respectively, for the standard PISCES-FFGM run (plain line) and the two sensitivity experiments: PISCES-GM (dashed line), and PISCES-v2 (dotted line).

anomalies from 100 m to the seafloor is observed (Figure 6c,f), yet with a reduced intensity.

Thus, due to the strong trophic amplification of macrozooplankton and the major contribution of their carcasses and fecal pellets to the deep POC flux, the supply of organic matter to the benthos is projected to be strongly reduced in response to climate change. However, this reduction is mitigated at the global scale by the representation of FFGM, which, due to a lower trophic amplification, induces a slightly lower decrease in POC flux at the bottom than in the upper ocean. This effect is particularly important in the low-latitude oligotrophic areas (Figure 6, Table S5) in which FFGM dominate macrozooplankton by a factor of 2 (Figure 4), so that FFGM have a buffering role on the deep POC flux in these areas strongly affected by climate change.

3.3 | Anthropogenic carbon uptake

The PISCES-FFGM integrated anthropogenic carbon uptake over the historical period (1850–2014) of 142.28 PgC is consistent with the estimate from the Global Carbon Budget 2021 of 150±30 PgC (Figure 3c, Friedlingstein et al., 2022). Over the whole simulation period (1850–2100), the ocean anthropogenic carbon uptake remains almost unchanged when FFGM are removed (Figure 3d) and even compared with the PISCES-v2 version: under RCP8.5 (resp. RCP2.6) scenario the integrated uptake is 554.27 PgC (resp. 308.02 PgC), that is, +0.04% (resp. +0.21%) compared with PISCES-GM and −0.40% (resp +0.23%) compared with PISCES-v2. Thus, the addition of two new macrozooplankton compartments to the PISCES marine biogeochemical model has virtually no impact on the anthropogenic carbon flux to the ocean in either the historical simulations or the projections.

4 | DISCUSSION AND PERSPECTIVES

In this study, we provide a model-based estimate of potential community shifts in macrozooplankton composition and evaluate for the first time their effects on benthic food supply and carbon cycling under RCP2.6 and RCP8.5 scenarios. The model, which explicitly represents one gelatinous (FFGM) and one nongelatinous (GM) macrozooplankton, shows that macrozooplankton biomass declines under climate-change scenarios, but that gelatinous zooplankton are less affected than nongelatinous zooplankton, consistent with the jellification hypothesis (Parsons & Lalli, 2002; Roux et al., 2013). Inclusion of those organisms has a limited effect on anthropogenic carbon uptake over the 21st century, but it consequently affects the projected changes in deep particulate carbon fluxes and composition, with potential implications for benthic ecosystems and deep carbon sequestration.

4.1 | Model caveats

Although this study provides an overview of the impacts of FFGMs on biogeochemical processes in a context of climate change, the model used here has limitations and simplifying assumptions that the reader should bear in mind when interpreting the results.

First, PISCES-FFGM represents a simplified marine planktonic ecosystem with a limited number of plankton functional types (two phytoplankton and four zooplankton), especially when compared to models that already include gelatinous zooplankton (ZooMSS, COBALT and PLANKTOM11 simulate 10, 10, and 11 PFTs, respectively; Heneghan et al., 2023; Luo et al., 2022; Wright et al., 2021). Consequently, our PISCES-FFGM model probably has a limited capacity to quantify in detail the impacts of climate change on the trophic structure of the planktonic ecosystem. For example, the FFGM PFT (i.e., pelagic tunicates) does not take appendicularians into account. Although it has been suggested that these organisms contribute less to the production of detritus than large tunicates (Luo et al., 2022), they have access to even smaller prey than other FFGMs, which allows them to shorten food chains even further. This "appendicularian shunt" is likely to affect the trophic structure in a context of climate change and should be taken into account to properly study the future impact of tunicates on the ecosystem structure (Heneghan et al., 2023; Jaspers et al., 2023). Also, there are critical gaps in knowledge on the impact of appendicularians on carbon export, their discarded houses, absent in larger tunicates, are likely to significantly contribute to the carbon cycle (Jaspers et al., 2023) and should be considered in further model developments. That said, the highly simplistic ecosystem framework used here has enabled an explicit representation of both FFGM carcasses and fecal pellets, leading to a comprehensive analysis of the potential impacts of FFGM on deep carbon export and sequestration.

Second, the physical framework used here is based on an offline approach. This approach limits the computational costs of the simulations, but prevents the inclusion of biogeochemical feedbacks on ocean physics (Lengaigne et al., 2007). In addition, the main drawback of this offline approach is probably linked to the fact that we use temporal interpolation of the monthly averages of all the physical fields (e.g., temperature, ocean currents, and depth of the mixing layer) to force the biogeochemical model. This approach therefore smoothes out all the effects of high-frequency events and prevents any analysis of the response of biogeochemistry and ecosystems to this high-frequency variability.

Third, as noted in Clerc, Bopp, Benedetti, et al. (2023), model evaluation is difficult due to the scarcity and patchiness of macrozooplankton observations. In addition, the ocean physics used here comes from the IPSL ESM (Boucher et al., 2020) and has larger biases than the forcing used in Clerc, Bopp, Benedetti, et al. (2023). Consequently, the performance of PISCES-FFGM evaluated in comparison with the observation datasets AtlantECO for pelagic tunicates (Clerc, Bopp, Benedetti, et al., 2023) and MAREDAT for total macrozooplankton (Moriarty et al., 2013) is degraded compared with the scores indicated in Clerc, Bopp, Benedetti, et al. (2023; see Table S6). Although the model only partially reproduces the regional contrasts of the macrozooplankton biomasses reconstructed from the observations, the order of magnitude of the simulated biomasses remains consistent with the observations, with the exception of the Arctic where the data coverage is extremely low (<2% for FFGM; Table S6, Text S1). The ratios between FFGM and macrozooplankton biomasses are also consistent with what is shown in Clerc, Bopp, Benedetti, et al. (2023; Table S6, Text S1). In conclusion, the projected evolution of the carbon cycle and the impacts on the ecosystem must here be interpreted as a proof of concept rather than a quantitative projection of the future ocean.

4.2 | Toward a more gelatinous ocean?

Under RCP8.5 scenario, our results show that macrozooplankton will be strongly affected by climate change (−12% biomass for GM and −15.1% for FFGM). Simulated increased stratification limits nutrient supply and induces a 9% decline in phytoplankton biomass at the end of the 21st century. Due to trophic amplification, macrozooplankton biomass declines are amplified compared with phytoplankton. An opposite trend is observed at high latitudes, but the mid- and low-latitude oceans drive at the global scale the projected decline in biomass and the trophic amplification, consistent with previous studies (Chust et al., 2014; Kwiatkowski et al., 2019). The inclusion of an additional trophic level (macrozooplankton) allows trophic amplification to go one step further, but the projected decrease in total zooplankton biomasses remains within the range of the CMIP5 (−13.6 ± 3.0% in Kwiatkowski et al., 2019) and CMIP6 (−9.0 ± 8.9% in Cooley et al. 2022; Kwiatkowski et al. 2020) models.

Macrozooplankton composition is also affected by climate change: FFGM are less affected than GM due to their feeding mode that gives them access to small preys and to the expansion of low-productive areas in which they are favored over GM (simulated biomass decline per degree of warming is −3.5% for GM and −2.8% for FFGM). It implies that the flow of NPP that goes through macrozooplankton tends to be preferentially directed to FFGM ("gelatinous pathway") and not to GM ("crustacean pathway"). The direction of the effect is consistent with what has been hypothesized (Clerc, Bopp, Benedetti, et al., 2023; Luo et al., 2022; Sutherland & Thompson, 2022) and quantified (Heneghan et al., 2023). As a consequence, as FFGM provide a direct pathway from small phytoplankton to higher trophic levels, they could buffer the expected climate change-induced lengthening of food webs (Heneghan et al., 2023). A coupled version of PISCES with a higher trophic level model, such as APECOSM (Dupont et al., 2022; Maury, 2010), would be relevant to properly quantify this effect. Moreover, simulated zooplankton trends are not spatially homogeneous. In particular, in the SO, where our model projects an increase in GM over FFGM, the projection is opposite to that described for the ratio of krill (included in GM) to salps (included in FFGM; Atkinson et al., 2004; Groeneveld et al., 2020). Nevertheless, at the scale of the SO, many uncertainties remain about the effects of climate change and the biotic and abiotic conditions favoring the proliferation of salps or krill (Atkinson et al., 2004, 2019; Cox et al., 2018).

The conservative and highly simplistic assumptions in our model (growth rate and temperature dependency identical for GM and FFGM, no life cycle representation) can however explain these low variations. An improved understanding of the ecological and environmental factors driving bloom-and-burst dynamics of FFGM populations is key before accurately model their complexity in an ocean ecosystem model (Clerc, Bopp, Benedetti, et al., 2023; Pitt et al., 2014). Also, contrary to cnidarians, large pelagic tunicates are open ocean species (Henschke et al., 2016). Coastal and shallow ecosystems are confronted with multiple other anthropogenic stressors (e.g., eutrophication and fisheries; Harley et al., 2006) that are more likely to provide environmental conditions that would favor gelatinous zooplankton over other organisms (Lucas et al., 2014; Purcell, 2012). Still, large pelagic tunicates could also proliferate in coastal environments, which are not properly resolved in our model due to its coarse spatial resolution, as many unprecedented swarms in coastal areas have been reported during the last decades (Abdelsalam et al., 2022; Boero et al., 2013; Li et al., 2016). Lastly, an explicit representation of UTL is likely to introduce top-down climate-change impacts (Dupont et al., 2022), and differential predation by UTL on both macrozooplankton groups is likely to affect their response to climate change as suggested by Parsons and Lalli (2002).

4.3 | Macrozooplankton impacts on deep carbon export and benthic food supply

Because of their large and dense carcasses and fecal pellets, GM and FFGM efficiently transfer POC to the ocean floor. This has two effects: macrozooplankton-produced particles dominate the POC flux to the seafloor, but they also drive the effects of climate change on these fluxes. At the global scale, these fluxes are greatly impacted by climate change due to trophic amplification, that is, a 14.9% (resp. −2.7%) reduction in their magnitude under RCP8.5 (resp. RCP2.6) scenario for the end of the 21st century. Spatial patterns of the anomalies are similar to those projected by Jones et al. (2014) and Sweetman et al. (2017) and are largely driven by changes in surface productivity, with positive anomalies at high latitudes and negative anomalies at low latitudes. However, our global projected seafloor (>1000 m) POC flux decline is much lower than what was projected by Yool et al. (2017; −29.3% under RCP8.5, −8.7% under RCP2.6). In fact, their larger decline is similar to that projected for seafloor fluxes by small organic carbon particles in PISCES-v2 (−25.5%, under RCP8.5, Table S4, −6.8% under RCP2.6). Also, the seafloor (>1000 m) historical POC flux value of 643 TgC year^{-1} projected by PISCES-FFGM is similar to their value of 710 TgC year^{-1}. Deep climate-change impacts on POC fluxes under both RCP8.5 and RCP2.6 scenarios are mitigated by the representation of FFGM at the global scale, which, due to a lower trophic amplification than GM, induces a slightly lower decrease in POC flux at depth than in the surface ocean. An opposite vertical trend is projected in Yool et al. (2017) and in PISCES-v2. This effect is particularly important in low-latitude oligotrophic areas in which FFGM dominates macrozooplankton by a factor of 2. Therefore, FFGM play a buffering role on the deep POC flux in these areas strongly affected by climate change.

Beyond the attenuation of the projected anomalies in POC fluxes to the seafloor due to the addition of macrozooplankton, and in particular FFGM, our study gives some insights in the potential drivers of POC fluxes to the seafloor and on the associated benthic food supply (Henschke et al., 2013). It provides deep POC flux fields that could be used in benthos models (e.g., Jones et al., 2014; Kelly-Gerreyn et al., 2014; Yool et al., 2017) to better project the benthic biomass evolution under climate change by distinguishing anomalies for six types of particles (small, large, GM and FFGM carcasses and fecal pellets). Direct evidence of gelatinous zooplankton carcasses and fecal pellets representing a significant portion of benthic food supply supports this claim (Pfannkuche & Lochte, 1993; Smith et al., 2014; Sweetman et al., 2014). In particular, a large salp swarm in the northeastern Pacific in the spring of 2012 resulted in major deposition of carcasses and fecal pellets on the seafloor, so that a dominant megafauna species increased sevenfold in density within a 2-month delay (Smith et al., 2014).

4.4 | Macrozooplankton impacts on the anthropogenic carbon uptake

The effects of adding macrozooplankton (GM and FFGM) in a ocean biogeochemical model on the ocean carbon cycle have been described in Clerc, Bopp, Benedetti, et al. (2023) and Luo et al. (2022). In brief, the inclusion of macrozooplankton and the associated production of carcasses and fecal pellets redistributes particles between the different particle compartments in the surface ocean, with more of large particles, without significantly altering the total amount of particulate carbon exported from the surface ocean. This change in particle composition however is explaining the major role that macrozooplankton play in carbon export to the deep ocean, due to higher transfer efficiency and resulting into higher deep carbon fluxes at 1000 m and at the sea floor. This suggests a deepening of the remineralization depth (depth at which the sinking carbon is converted back to carbon dioxide) in a model that includes macrozooplankton, explained by higher mean particle sinking speeds. Kwon et al. (2009) showed that a modest change in the remineralization depth in a 3D biogeochemical model could have a substantial impact on atmospheric carbon dioxide concentrations as a result of the redistribution of remineralized carbon from intermediate waters to bottom waters.

The effects of climate change on POC fluxes in the water column are modulated by the introduction of macrozooplankton (GM and FFGM). At 100 m, the addition of macrozooplankton amplifies the POC flux decline due to changes in ecosystem composition (Section 3.3). At 1000 m and at the seafloor, the addition of FFGM is most important and attenuates the POC flux decrease (Section 3.3). Yet, the effects of GM and FFGM on anthropogenic carbon uptake are small, that is, the uptake of anthropogenic carbon is almost identical in all model versions for each of the scenarios (Section 3.3). This uptake results mostly from the transport of that carbon via the physical pump (Sarmiento & Gruber, 2006), but is modulated by potential changes in the biological pump that affect the dissolved inorganic carbon gradient. The impact on the biological pump through the introduction of GM and FFGM in our simulation however does not affect anthropogenic carbon uptake over the time scales addressed here. This is not surprising, and similar results have been found for other biological processes over the same time scales, for example, potential feedbacks from high-trophic levels (Dupont et al., 2022) or changes in N_2-fixation (Bopp et al., 2022).

That said, the modifications of the biological pump induced by changes in macrozooplankton composition could have larger effects on ocean carbon uptake on longer time scales. The POC flux at 1000 m has been recently suggested as a good proxy of long-term anthropogenic carbon sequestration (Wilson et al., 2022): An idealized simulation shows a quasilinear positive relationship between changes in POC fluxes at 1000 m and the ocean carbon sink. Thus, over longer time scales (multiple centuries), we could expect a lower ocean carbon sink in PISCES-GM compared with PISCES-FFGM and an even lower sink in PISCES-v2.

Future changes in the biological pump remain highly uncertain, and the increasing complexity of biogeochemical models results in increasing uncertainties on the impacts of climate change on export: The POC flux at 100 m is projected to decline by −1% to −12% in CMIP5 under RCP8.5 scenario and −2.1% to −21.5% in CMIP6 under SSP5-8.5 scenario (WGI AR6 5.4.4.2, tab. 3.24, Cooley et al., 2022). In CMIP5, changes in stratification and reduced nutrient supply dominate (Bindoff et al., 2019; Fu et al., 2016) while in CMIP6, more complex biological processes (Bopp et al., 2022; Le Quéré et al., 2016; Séférian et al., 2020; Wright et al., 2021) increase the associated uncertainties. Yet, there are still numerous overlooked processes (Boyd et al., 2019), for instance diurnal vertical migrations. Filter-feeding gelatinous zooplankton are one of these largely overlooked processes in climate models. This study provides insights on large pelagic tunicates impacts on the biological carbon pump under climate change and reveals their potential importance for deep carbon sequestration.

AUTHOR CONTRIBUTIONS

Corentin Clerc, Laurent Bopp, and Olivier Aumont conceived the study. Corentin Clerc, Olivier Aumont, and Laurent Bopp developed the model for this study. Corentin Clerc processed model outputs and performed the analysis. All authors contributed to the paper.

ACKNOWLEDGEMENTS

We are very grateful to Lars Stemmann, Olivier Maury, Jean-Christophe Poggiale, and Fabien Lombard for the insightful comments during the development of this paper and to Christian Ethé and Olivier Torres for setting up the model configuration. This project used the HPC resources of TGCC under the allocation A13 (project no. gen0040) provided by GENCI (Grand Equipement National de Calcul Intensif). This study benefited from the ESPRI (Ensemble de Services Pour la Recherche l'IPSL) computing and data center (https://mesocentre.ipsl.fr, last accessed 17 November 2022), which is supported by CNRS, Sorbonne Université, Ecole Polytechnique, and CNES and through national and international grants. This study has received funding from the Agence Nationale de la Recherche (grant no. ANR-17-CE32-0008; CIGOEF). Laurent Bopp acknowledges support from the European Union's Horizon 2020 research and innovation COMFORT (grant agreement no. 820989), ESM2025 (grant agreement no. 101003536) and from the Chaire ENS-Chanel.

CONFLICT OF INTEREST STATEMENT

The contact author has declared that none of the authors has any competing interests.

DATA AVAILABILITY STATEMENT

The simulation outputs that support the findings of this study are openly available in Zenodo at https://doi.org/10.5281/zenodo.8306115 (Clerc, Bopp, & Aumont, 2023).

ORCID

Corentin Clerc https://orcid.org/0000-0002-8436-4391

REFERENCES

Abdelsalam, K. M., Ramadan, S. E., & Ahmed, H. O. (2022). First record of a swarm of *Thalia democratica* (Chordata: Tunicata) in the Egyptian Mediterranean coast. *The Egyptian Journal of Aquatic Research*, *48*, 131–135.

Acuña, J. L., López-Urrutia, Á., & Colin, S. (2011). Faking giants: The evolution of high prey clearance rates in jellyfishes. *Science*, *333*, 1627–1629.

Armengol, L., Calbet, A., Franchy, G., Rodríguez-Santos, A., & Hernández-León, S. (2019). Planktonic food web structure and trophic transfer efficiency along a productivity gradient in the tropical and subtropical Atlantic Ocean. *Scientific Reports*, *9*, 1–19.

Ates, R. M. (2017). Benthic scavengers and predators of jellyfish, material for a review. *Plankton and Benthos Research*, *12*, 71–77.

Atkinson, A., Hill, S. L., Pakhomov, E. A., Siegel, V., Reiss, C. S., Loeb, V. J., Steinberg, D. K., Schmidt, K., Tarling, G. A., Gerrish, L., & Sailley, S. F. (2019). Krill (*Euphausia superba*) distribution contracts southward during rapid regional warming. *Nature Climate Change*, *9*, 142–147.

Atkinson, A., Siegel, V., Pakhomov, E., & Rothery, P. (2004). Long-term decline in krill stock and increase in salps within the southern ocean. *Nature*, *432*, 100–103.

Aumont, O., Ethé, C., Tagliabue, A., Bopp, L., & Gehlen, M. (2015). PISCES-v2: An ocean biogeochemical model for carbon and ecosystem studies. *Geoscientific Model Development*, *8*, 2465–2513.

Bindoff, N. L., Cheung, W. W. L., Kairo, J. G., Arstegui, J., Guinder, V. A., Hallberg, R., Hilmi, N., Jiao, N., Karim, M. S., Levin, L., O'Donoghue, S., Purca Cuicapusa, S. R., Rinkevich, B., Suga, T., Tagliabue, A., & Williamson, P. (2019). Changing ocean, marine ecosystems, and dependent communities. In H.-O. Pörtner, D. C. Roberts, V. Masson-Delmotte, P. Zhai, M. Tignor, E. Poloczanska, K. Mintenbeck, A. Alegría, M. Nicolai, A. Okem, J. Petzold, B. Rama, N. M. Weyer (Eds.), *IPCC special report on the ocean and cryosphere in a changing climate* (pp. 477–587). Cambridge University Press.

Boero, F., Belmonte, G., Bracale, R., Fraschetti, S., Piraino, S., & Zampardi, S. (2013). A salp bloom (Tunicata, Thaliacea) along the Apulian coast and in the Otranto Channel between March-May 2013. *F1000Research*, *2*, 181.

Bopp, L., Aumont, O., Kwiatkowski, L., Clerc, C., Dupont, L., Ethé, C., Gorgues, T., Séférian, R., & Tagliabue, A. (2022). Diazotrophy as a key driver of the response of marine net primary productivity to climate change. *Biogeosciences*, *19*, 4267–4285. https://bg.copernicus.org/articles/19/4267/2022/

Boucher, O., Servonnat, J., Albright, A. L., Aumont, O., Balkanski, Y., Bastrikov, V., Bekki, S., Bonnet, R., Bony, S., Bopp, L., Braconnot, P., Brockmann, P., Cadule, P., Caubel, A., Cheruy, F., Codron, F., Cozic, A., Cugnet, D., D'Andrea, F., … Vuichard, N. (2020). Presentation and evaluation of the IPSL-CM6A-LR climate model. *Journal of Advances in Modeling Earth Systems*, *12*, e2019MS002010.

Boyd, P. W., Claustre, H., Levy, M., Siegel, D. A., & Weber, T. (2019). Multi-faceted particle pumps drive carbon sequestration in the ocean. *Nature*, *568*, 327–335.

Brotz, L., Cheung, W. W., Kleisner, K., Pakhomov, E., & Pauly, D. (2012). Increasing jellyfish populations: Trends in large marine ecosystems. In *Jellyfish blooms IV* (pp. 3–20). Springer.

Chelsky, A., Pitt, K. A., & Welsh, D. T. (2015). Biogeochemical implications of decomposing jellyfish blooms in a changing climate. *Estuarine, Coastal and Shelf Science*, *154*, 77–83.

Chust, G., Allen, J. I., Bopp, L., Schrum, C., Holt, J., Tsiaras, K., Zavatarelli, M., Chifflet, M., Cannaby, H., Dadou, I., Daewel, U., Wakelin, S. L., Machu, E., Pushpadas, D., Butenschon, M., Artioli, Y., Petihakis, G., Smith, C., Garçon, V., … Irigoien, X. (2014). Biomass changes and trophic amplification of plankton in a warmer ocean. *Global Change Biology*, *20*, 2124–2139.

Clerc, C., Bopp, L., & Aumont, O. (2023). Supplementary material for "Filter-feeding gelatinous macrozooplankton response to climate change and implications for benthic food supply and global carbon cycle". https://doi.org/10.5281/zenodo.8306115

Clerc, C., Bopp, L., Benedetti, F., Vogt, M., & Aumont, O. (2023). Including filter-feeding gelatinous macrozooplankton in a global marine biogeochemical model: Model–data comparison and impact on the ocean carbon cycle. *Biogeosciences*, *20*, 869–895. https://bg.copernicus.org/articles/20/869/2023/

Condon, R. H., Duarte, C. M., Pitt, K. A., Robinson, K. L., Lucas, C. H., Sutherland, K. R., Mianzan, H. W., Bogeberg, M., Purcell, J. E., Decker, M. B., Uye, S. I., Madin, L. P., Brodeur, R. D., Haddock, S. H. D., Malej, A., Parry, G. D., Eriksen, E., Quiñones, J., Acha, M., … Graham, W. M. (2013). Recurrent jellyfish blooms are a consequence of global oscillations. *Proceedings of the National Academy of Sciences of the United States of America*, *110*, 1000–1005.

Condon, R. H., Graham, W. M., Duarte, C. M., Pitt, K. A., Lucas, C. H., Haddock, S. H., Sutherland, K. R., Robinson, K. L., Dawson, M. N., Decker, M. B., Mills, C. E., Purcell, J. E., Malej, A., Mianzan, H., Uye, S.-I., Gelcich, S., & Madin, L. P. (2012). Questioning the rise of gelatinous zooplankton in the world's oceans. *Bioscience*, *62*, 160–169.

Condon, R. H., Lucas, C. H., Pitt, K. A., & Uye, S.-I. (2014). Jellyfish blooms and ecological interactions. *Marine Ecology Progress Series*, *510*, 109–110.

Cooley, S., Schoeman, D., Bopp, L., Boyd, P., Donner, S., Ito, S.-I., Kiessling, W., Martinetto, P., Ojea, E., Racault, M.-F., Rost, B., Skern-Mauritzen, M., & Yemane Ghebrehiwet, D. (2022). Oceans and coastal ecosystems and their services. In *IPCC AR6 WGII*. Cambridge University Press.

Cox, M. J., Candy, S., de la Mare, W. K., Nicol, S., Kawaguchi, S., & Gales, N. (2018). No evidence for a decline in the density of Antarctic krill *Euphausia superba* Dana, 1850, in the Southwest Atlantic sector between 1976 and 2016. *Journal of Crustacean Biology*, *38*, 656–661.

Décima, M., Stukel, M. R., Nodder, S. D., Gutiérrez-Rodrguez, A., Selph, K. E., Dos Santos, A. L., Safi, K., Kelly, T. B., Deans, F., Morales, S. E., Baltar, F., Latasa, M., Gorbunov, M. Y., & Pinkerton, M. (2023). Salp blooms drive strong increases in passive carbon export in the southern ocean. *Nature Communications*, *14*, 425.

DeVries, T., Holzer, M., & Primeau, F. (2017). Recent increase in oceanic carbon uptake driven by weaker upper-ocean overturning. *Nature*, *542*, 215–218.

Dufresne, J.-L., Foujols, M.-A., Denvil, S., Caubel, A., Marti, O., Aumont, O., Balkanski, Y., Bekki, S., Bellenger, H., Benshila, R., Bony, S., Bopp, L., Braconnot, P., Brockmann, P., Cadule, P., Cheruy, F., Codron, F., Cozic, A., Cugnet, D., … Vuichard, N. (2013). Climate change projections using the IPSL-CM5 earth system model: From CMIP3 TO CMIP5. *Climate Dynamics*, *40*, 2123–2165.

Dupont, L., Le Mézo, P., Aumont, O., Bopp, L., Clerc, C., Ethé, C., & Maury, O. (2022). High trophic level feedbacks on global ocean carbon uptake and marine ecosystem dynamics under climate change. *Global Change Biology*, *29*, 1545–1556.

Everett, J., Heneghan, R., Blanchard, J., Suthers, I., Pakhomov, E., Sykes, P., Schoeman, D., Baird, M., Basedow, S. L., Błachowiak-Samołyk, K. Heath, M., Hopcroft, R., Huggett, J., Huret, M., Kimmel, D., Labat, J, Lopes, R., Marcolin, C., Nogueira, E. … Richardson, A. (2022). Self-organisation of zooplankton communities produces similar food chain lengths throughout the ocean.

Eyring, V., Bony, S., Meehl, G. A., Senior, C. A., Stevens, B., Stouffer, R. J., & Taylor, K. E. (2016). Overview of the coupled model intercomparison project phase 6 (CMIP6) experimental design and organization. *Geoscientific Model Development*, *9*, 1937–1958.

Francis, T. B., Scheuerell, M. D., Brodeur, R. D., Levin, P. S., Ruzicka, J. J., Tolimieri, N., & Peterson, W. T. (2012). Climate shifts the interaction web of a marine plankton community. *Global Change Biology*, *18*, 2498–2508.

Friedlingstein, P., Jones, M. W., O'Sullivan, M., Andrew, R. M., Bakker, D. C., Hauck, J., Le Quéré, C., Peters, G. P., Peters, W., Pongratz, J., Sitch, S., Canadell, J. G., Ciais, P., Jackson, R. B., Alin, S. R., Anthoni, P., Bates, N. R., Becker, M., Bellouin, N., … Zeng, J. (2022). Global carbon budget 2021. *Earth System Science Data*, *14*, 1917–2005.

Fu, W., Randerson, J. T., & Moore, J. K. (2016). Climate change impacts on net primary production (NPP) and export production (EP) regulated by increasing stratification and phytoplankton community structure in the CMIP5 models. *Biogeosciences*, *13*, 5151–5170.

Gibbons, M. J., & Richardson, A. J. (2013). Beyond the jellyfish joyride and global oscillations: Advancing jellyfish research. *Journal of Plankton Research*, *35*, 929–938.

Groeneveld, J., Berger, U., Henschke, N., Pakhomov, E. A., Reiss, C. S., & Meyer, B. (2020). Blooms of a key grazer in the Southern Ocean–An individual-based model of *Salpa thompsoni*. *Progress in Oceanography*, *185*, 102339.

Harley, C. D., Randall Hughes, A., Hultgren, K. M., Miner, B. G., Sorte, C. J., Thornber, C. S., Rodriguez, L. F., Tomanek, L., & Williams, S. L. (2006). The impacts of climate change in coastal marine systems. *Ecology Letters*, *9*, 228–241.

Heneghan, R. F., Everett, J. D., Blanchard, J. L., Sykes, P., & Richardson, A. J. (2023). Climate-driven zooplankton shifts cause large-scale declines in food quality for fish. *Nature Climate Change*, *13*, 470–477.

Henschke, N., Bowden, D. A., Everett, J. D., Holmes, S. P., Kloser, R. J., Lee, R. W., & Suthers, I. M. (2013). Salp-falls in the Tasman Sea: A major food input to deep-sea benthos. *Marine Ecology Progress Series*, *491*, 165–175.

Henschke, N., Everett, J. D., Richardson, A. J., & Suthers, I. M. (2016). Rethinking the role of salps in the ocean. *Trends in Ecology & Evolution*, *31*, 720–733.

Jaspers, C., Hopcroft, R. R., Kiørboe, T., Lombard, F., López-Urrutia, Á., Everett, J. D., & Richardson, A. J. (2023). Gelatinous larvacean zooplankton can enhance trophic transfer and carbon sequestration. *Trends in Ecology & Evolution*, *38*, 980–993.

Jones, D. O., Yool, A., Wei, C.-L., Henson, S. A., Ruhl, H. A., Watson, R. A., & Gehlen, M. (2014). Global reductions in seafloor biomass in response to climate change. *Global Change Biology*, *20*, 1861–1872.

Kelly-Gerreyn, B., Martin, A., Bett, B., Anderson, T., Kaariainen, J., Main, C., Marcinko, C., & Yool, A. (2014). Benthic biomass size spectra in shelf and deep-sea sediments. *Biogeosciences*, *11*, 6401–6416.

Kwiatkowski, L., Aumont, O., & Bopp, L. (2019). Consistent trophic amplification of marine biomass declines under climate change. *Global Change Biology*, *25*, 218–229.

Kwiatkowski, L., Torres, O., Bopp, L., Aumont, O., Chamberlain, M., Christian, J. R., Dunne, J. P., Gehlen, M., Ilyina, T., John, J. G., Lenton, A., Li, H., Lovenduski, N. S., Orr, J. C., Palmieri, J., Santana-Falcón, Y., Schwinger, J., Séférian, R., Stock, C. A., … Ziehn, T. (2020). Twenty-first century ocean warming, acidification, deoxygenation, and upper-ocean nutrient and primary production decline from cmip6 model projections. *Biogeosciences*, *17*, 3439–3470.

Kwon, E. Y., Primeau, F., & Sarmiento, J. L. (2009). The impact of remineralization depth on the air–sea carbon balance. *Nature Geoscience*, *2*, 630–635.

Le Quéré, C., Buitenhuis, E. T., Moriarty, R., Alvain, S., Aumont, O., Bopp, L., Chollet, S., Enright, C., Franklin, D. J., Geider, R. J., Harrison, S. P., Hirst, A. G., Larsen, S., Legendre, L., Platt, T., Prentice, I. C., Rivkin, R. B., Sailley, S., Sathyendranath, S., … Vallina, S. M. (2016). Role of zooplankton dynamics for southern ocean phytoplankton biomass and global biogeochemical cycles. *Biogeosciences*, *13*, 4111–4133.

Lebrato, M., Mendes, P. d. J., Steinberg, D. K., Cartes, J. E., Jones, B. M., Birsa, L. M., Benavides, R., & Oschlies, A. (2013). Jelly biomass sinking speed reveals a fast carbon export mechanism. *Limnology and Oceanography*, *58*, 1113–1122.

Lebrato, M., Pahlow, M., Frost, J. R., Küter, M., de Jesus Mendes, P., Molinero, J.-C., & Oschlies, A. (2019). Sinking of gelatinous zooplankton biomass increases deep carbon transfer efficiency globally. *Global Biogeochemical Cycles*, *33*, 1764–1783.

Lebrato, M., Pitt, K. A., Sweetman, A. K., Jones, D. O., Cartes, J. E., Oschlies, A., Condon, R. H., Molinero, J. C., Adler, L., Gaillard, C., Domingo, L., & Billet, D. S. M. (2012). Jelly-falls historic and recent observations: A review to drive future research directions. *Hydrobiologia*, *690*, 227–245.

Lengaigne, M., Menkes, C., Aumont, O., Gorgues, T., Bopp, L., André, J.-M., & Madec, G. (2007). Influence of the oceanic biology on the tropical pacific climate in a coupled general circulation model. *Climate Dynamics*, *28*, 503–516.

Li, K., Doubleday, A. J., Galbraith, M. D., & Hopcroft, R. R. (2016). High abundance of salps in the Coastal Gulf of Alaska during 2011: A first record of bloom occurrence for the Northern Gulf. *Deep Sea Research Part II: Topical Studies in Oceanography*, *132*, 136–145.

Lucas, C. H., Jones, D. O., Hollyhead, C. J., Condon, R. H., Duarte, C. M., Graham, W. M., Robinson, K. L., Pitt, K. A., Schildhauer, M., & Regetz, J. (2014). Gelatinous zooplankton biomass in the global oceans: Geographic variation and environmental drivers. *Global Ecology and Biogeography*, *23*, 701–714.

Luo, J. Y., Condon, R. H., Stock, C. A., Duarte, C. M., Lucas, C. H., Pitt, K. A., & Cowen, R. K. (2020). Gelatinous zooplankton-mediated carbon flows in the global oceans: A data-driven modeling study. *Global Biogeochemical Cycles*, *34*, e2020GB006704.

Luo, J. Y., Stock, C. A., Henschke, N., Dunne, J. P., & O'Brien, T. D. (2022). Global ecological and biogeochemical impacts of pelagic tunicates. *Progress in Oceanography*, *205*, 102822.

Madec, G. (2008). *Nemo reference manual, ocean dynamic component: Nemo–opa, note du pôle de modélisation*. Technical Report 27, Note du pôle de modélisation. Institut Pierre Simmon.

Maury, O. (2010). An overview of apecosm, a spatialized mass balanced "apex predators ecosystem model" to study physiologically structured tuna population dynamics in their ecosystem. *Progress in Oceanography*, *84*, 113–117.

McClain, C. R., Allen, A. P., Tittensor, D. P., & Rex, M. A. (2012). Energetics of life on the deep seafloor. *Proceedings of the National Academy of Sciences of the United States of America*, *109*, 15366–15371.

McKinley, G. A., Fay, A. R., Lovenduski, N. S., & Pilcher, D. J. (2017). Natural variability and anthropogenic trends in the ocean carbon sink. *Annual Review of Marine Science*, *9*, 125–150.

Moriarty, R., Buitenhuis, E., Le Quéré, C., & Gosselin, M.-P. (2013). Distribution of known macrozooplankton abundance and biomass in the global ocean. *Earth System Science Data*, *5*, 241–257.

Moss, R. H., Edmonds, J. A., Hibbard, K. A., Manning, M. R., Rose, S. K., van Vuuren, D. P., Carter, T. R., Emori, S., Kainuma, M., Kram, T., Meehl, G. A., Mitchell, J. F., Nakicenovic, N., Riahi, K., Smith, S. J., Stouffer, R. J., Thomson, A. M., Weyant, J. P., & Wilbanks, T. J. (2010). The next generation of scenarios for climate change research and assessment. *Nature*, *463*, 747–756.

Parsons, T., & Lalli, C. (2002). Jellyfish population explosions: Revisiting a hypothesis of possible causes. *La Mer*, *40*, 111–121.

Peter, K. H., & Sommer, U. (2013). Phytoplankton cell size reduction in response to warming mediated by nutrient limitation. *PLoS One*, *8*, e71528.

Pfannkuche, O., & Lochte, K. (1993). Open Ocean pelago-benthic coupling: Cyanobacteria as tracers of sedimenting salp faeces. *Deep Sea Research Part I: Oceanographic Research Papers*, *40*, 727–737.

Pitt, K. A., Budarf, A. C., Browne, J. G., & Condon, R. H. (2014). Bloom and bust: Why do blooms of jellyfish collapse? In K. A. Pitt & C. H. Lucas (Eds.), *Jellyfish blooms* (pp. 79–103). Springer.

Pitt, K. A., Lucas, C. H., Condon, R. H., Duarte, C. M., & Stewart-Koster, B. (2018). Claims that anthropogenic stressors facilitate jellyfish blooms have been amplified beyond the available evidence: A systematic review. *Frontiers in Marine Science*, *5*, 451.

Purcell, J. E. (2012). Jellyfish and ctenophore blooms coincide with human proliferations and environmental perturbations. *Annual Review of Marine Science*, *4*, 209–235.

Purcell, J. E., Uye, S.-i., & Lo, W.-T. (2007). Anthropogenic causes of jellyfish blooms and their direct consequences for humans: A review. *Marine Ecology Progress Series*, *350*, 153–174.

Richardson, A. J., Bakun, A., Hays, G. C., & Gibbons, M. J. (2009). The jellyfish joyride: Causes, consequences and management responses to a more gelatinous future. *Trends in Ecology & Evolution*, *24*, 312–322.

Richardson, A. J., & Gibbons, M. J. (2008). Are jellyfish increasing in response to ocean acidification? *Limnology and Oceanography*, *53*, 2040–2045.

Roux, J.-P., van der Lingen, C. D., Gibbons, M. J., Moroff, N. E., Shannon, L. J., Smith, A. D., & Cury, P. M. (2013). Jellyfication of marine ecosystems as a likely consequence of overfishing small pelagic fishes: Lessons from the Benguela. *Bulletin of Marine Science*, *89*, 249–284.

Sarmiento, J. L., & Gruber, N. (2006). *Ocean biogeochemical dynamics*. Princeton University Press. https://press.princeton.edu/titles/8223.html

Séférian, R., Berthet, S., Yool, A., Palmieri, J., Bopp, L., Tagliabue, A., Kwiatkowski, L., Aumont, O., Christian, J., Dunne, J., Gehlen, M., Ilyina, T., John, J. G., Li, H., Long, M. C., Luo, J. Y., Nakano, H., Romanou, A., Schwinger, J., … Yamamoto, A. (2020). Tracking improvement in simulated marine biogeochemistry between CMIP5 and CMIP6. *Current Climate Change Reports*, *6*, 95–119.

Smith, B. E., Ford, M. D., & Link, J. S. (2016). Bloom or bust: Synchrony in jellyfish abundance, fish consumption, benthic scavenger abundance, and environmental drivers across a continental shelf. *Fisheries Oceanography*, *25*, 500–514.

Smith, C. R., De Leo, F. C., Bernardino, A. F., Sweetman, A. K., & Arbizu, P. M. (2008). Abyssal food limitation, ecosystem structure and climate change. *Trends in Ecology & Evolution*, *23*, 518–528.

Smith, K. L., J., Sherman, A., Huffard, C., McGill, P., Henthorn, R., Von Thun, S., Ruhl, H., Kahru, M., & Ohman, M. (2014). Large salp bloom export from the upper ocean and benthic community response in the abyssal northeast pacific: Day to week resolution. *Limnology and Oceanography*, *59*, 745–757.

Stamieszkin, K., Pershing, A. J., Record, N. R., Pilskaln, C. H., Dam, H. G., & Feinberg, L. R. (2015). Size as the master trait in modeled copepod fecal pellet carbon flux. *Limnology and Oceanography*, *60*, 2090–2107.

Steinberg, D. K., & Landry, M. R. (2017). Zooplankton and the ocean carbon cycle. *Annual Review of Marine Science*, *9*, 413–444.

Steinberg, D. K., Stamieszkin, K., Maas, A. E., Durkin, C. A., Passow, U., Estapa, M. L., Omand, M. M., McDonnell, A. M. P., Karp-Boss, L., Galbraith, M., & Siegel, D. A. (2023). The outsized role of salps in carbon export in the subarctic northeast pacific ocean. *Global Biogeochemical Cycles*, *37*, e2022GB007523. https://doi.org/10.1029/2022GB007523

Stock, C., Dunne, J., & John, J. (2014). Drivers of trophic amplification of ocean productivity trends in a changing climate. *Biogeosciences*, *11*, 7125–7135.

Sutherland, K. R., Madin, L. P., & Stocker, R. (2010). Filtration of submicrometer particles by pelagic tunicates. *Proceedings of the National Academy of Sciences of the United States of America*, *107*, 15129–15134.

Sutherland, K. R., & Thompson, A. W. (2022). Pelagic tunicate grazing on marine microbes revealed by integrative approaches. *Limnology and Oceanography*, *67*, 102–121.

Sweetman, A. K., & Chapman, A. (2015). First assessment of flux rates of jellyfish carcasses (jelly-falls) to the benthos reveals the importance of gelatinous material for biological c-cycling in jellyfish-dominated ecosystems. *Frontiers in Marine Science*, *2*, 47.

Sweetman, A. K., Smith, C. R., Dale, T., & Jones, D. O. (2014). Rapid scavenging of jellyfish carcasses reveals the importance of gelatinous material to deep-sea food webs. *Proceedings of the Royal Society B: Biological Sciences*, *281*, 20142210.

Sweetman, A. K., Thurber, A. R., Smith, C. R., Levin, L. A., Mora, C., Wei, C.-L., Gooday, A. J., Jones, D. O., Rex, M., Yasuhara, M., Ingels, J., Ruhl, H. A., Frieder, C. A., Danovaro, R., Würzberg, L., Baco, A., Grupe, B. M., Pasulka, A., Meyer, K. S., … Roberts, J. M. (2017). Major impacts of climate change on deep-sea benthic ecosystems. *Elementa: Science of the Anthropocene*, *5*, 4. https://doi.org/10.1525/elementa.203

Taylor, K. E., Stouffer, R. J., & Meehl, G. A. (2012). An overview of CMIP5 and the experiment design. *Bulletin of the American Meteorological Society*, *93*, 485–498.

van der Reis, A., Jeffs, A., & Lavery, S. (2020). From feeding habits to food webs: Exploring the diet of an opportunistic benthic generalist. *Marine Ecology Progress Series*, *655*, 107–121.

Wilson, J. D., Andrews, O., Katavouta, A., de Melo Viríssimo, F., Death, R. M., Adloff, M., Baker, C. A., Blackledge, B., Goldsworth, F. W., Kennedy-Asser, A. T., Liu, Q., Sieradzan, K. R., Vosper, E., & Ying, R. (2022). The biological carbon pump in CMIP6 models: 21st century trends and uncertainties. *Proceedings of the National Academy of Sciences of the United States of America*, *119*, e2204369119.

Wright, R. M., Le Quéré, C., Buitenhuis, E., Pitois, S., & Gibbons, M. J. (2021). Role of jellyfish in the plankton ecosystem revealed using a global ocean biogeochemical model. *Biogeosciences*, *18*, 1291–1320.

Yool, A., Martin, A. P., Anderson, T. R., Bett, B. J., Jones, D. O., & Ruhl, H. A. (2017). Big in the benthos: Future change of seafloor community biomass in a global, body size-resolved model. *Global Change Biology*, *23*, 3554–3566.

Young, C. M., & Eckelbarger, K. J. (1994). *Reproduction, larval biology, and recruitment of the deep-sea benthos*. Columbia University Press.

SUPPORTING INFORMATION

Additional supporting information can be found online in the Supporting Information section at the end of this article.

How to cite this article: Clerc, C., Aumont, O., & Bopp, L. (2023). Filter-feeding gelatinous macrozooplankton response to climate change and implications for benthic food supply and global carbon cycle. *Global Change Biology*, *29*, 6383–6398. https://doi.org/10.1111/gcb.16942